SEISMIC PERFORMANCE OF MULTI-STORY SHEARWALL WITH AN ADJACENT FRAME CONSIDERING UPLIFT OF FOUNDATION

Kyohei Mori[1], Kyohei Murakami[2], Masanobu Sakashita[3], Susumu Kono[4] and Hitoshi Tanaka[5]

[1] *Graduate Student, Dept. of Architectural Engineering , Kyoto University*
[2] *Structural Engineer, Kajima Co.*
[3] *Assistant Professor, Dept. of Architecture and Architectural Engineering, Kyoto University*
[4] *Associate Professor, Dept. of Architecture and Architectural Engineering, Kyoto University*
[5] *Professor, Disaster Prevention research Institute, Kyoto University*
Email: rc.mori@archi.kyoto-u.ac.jp, sakashita@archi.kyoto-u.ac.jp , kono@archi.kyoto-u.ac.jp

ABSTRACT :

Reinforced concrete wall-frame structures are widely used for buildings. When such structures are subjected to severe earthquakes, rocking and sway motions can be observed at the base of these structures. As a result, foundations supporting rigid structural wall could be uplifted under certain circumstances. It is widely known that the uplift of foundations reduces the damage of structural wall but additional rotation of structural wall causes significant damage to the adjacent frame. The experimental studies dealing with such foundation uplift are not enough so far to establish a rational evaluation method for the performance based design. In order to study the basic performance relating to the uplift of structural walls, a static loading test was conducted using a 40% scale specimen consisting of a multi-story structural wall and an adjacent frame. Based on the test results, restoring force characteristics, energy dissipation capacity, etc. were evaluated, and the shear resisting mechanism was assessed to explain the observed damage propagation. The foundation of the test specimen was free to uplift and the applied horizontal shear force was equilibrated by friction between the specimen and the reaction floor. The damage of the specimen concentrated on the adjacent frame and the structural wall had a minor damage with few cracks. A frame analysis considering the uplift of foundation was also conducted, where the numerical model accurately simulated the envelope curve of the restoring force versus drift angle relations.

KEYWORDS: Foundation Uplift, RC Structural Wall, Frame Adjacent to Structural Wall, Frame Analysis, Restoring Force Characteristic

1. INTRODUCTION

RC structural walls are widely used in the building design to provide large shear stiffness and shear capacity against the seismic lateral load. However, it is not easy to adequately evaluate the stiffness and the resulting deformation of structure when the structural walls are constructed in combination with structural frames. This is because rocking action is likely to occur at the base of the structural wall part, possibly with uplift, when such structures are subjected to severe earthquakes. In this case, the adjacent frame is enforced to deform significantly to accommodate the large base rotation of the structural wall. Since the rocking wall dose not carry as much load as no-rocking wall, the adjacent frame has to carry more load and may experience further damage.

Recently performance evaluation procedures have come to be practiced. In these procedures, it is important to relate the response of structures with the damage level of structures. Harden et al. numerically modeled uplifting of foundations of rigid structural walls to account for the overall force-deformation behaviors [1]. They reported that the current suggestions [2] for relations between the stress ratio, R, and the displacement ratio, C_1, are highly unconservative when the uplifting foundation are anticipated, and proposed to revise the C_1-R relations for uplifting foundations. However, there is not enough experimental data dealing with foundation uplift to establish the performance evaluation procedures. More detailed information, such as cracked region of frame members or crack widths in accordance with the base rotational level of the attached

walls is required. In this study, static loading test, with a 3-story structural wall with an adjacent frame on one side, was conducted allowing foundation uplift in order to study the basic structural performance related to the uplifting behavior.
Based on the test results, restoring force characteristics, energy dissipation capacity, etc. were evaluated referring to the observed damage progress, where the applicability of existing damage evaluation procedures was also investigated. The experiment consists of two loading stages. The first loading stage was performed by permitting the foundation uplift. The second loading stage was conducted without permitting the foundation uplift.

2. EXPERIMENTAL SETUP

2.1. Specimen

Figure 1 shows specimen configuration and Figure 2 shows section configurations and bar arrangements. Specimen configuration was determined from a typical 3-story building in Japan. It consisted of a multi-story structural wall and an adjacent frame and was scaled to 40%. To prevent overturning sideway, wide foundations were cast on each side of the foundation beams under the columns. Material properties are shown in Table 1 and types of reinforcement are shown in Table 2. The structural wall was designed according to the Japanese design guidelines [3] so as to make the structural wall yield in flexure at first and finally fail in shear.

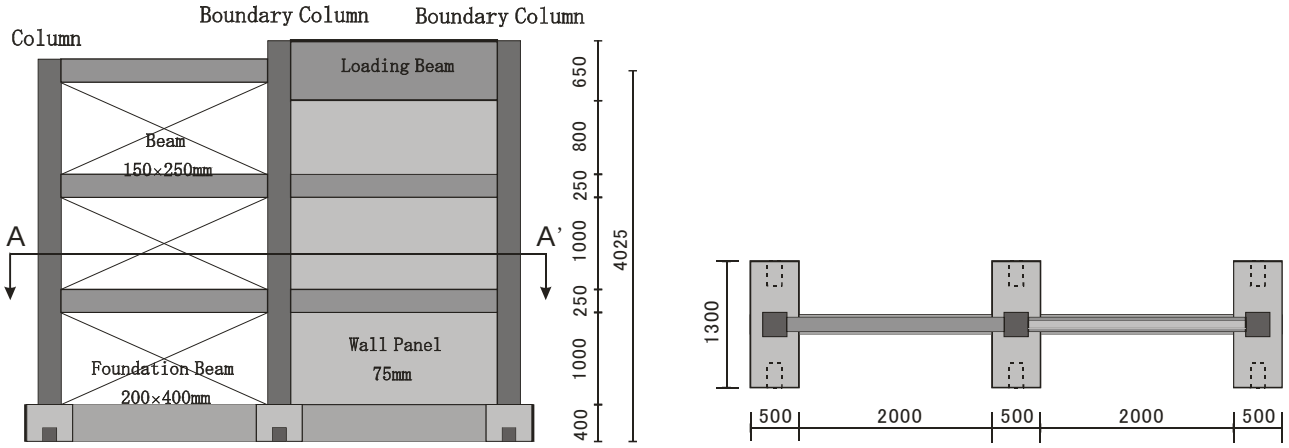

(a) Elevation **(b) A-A' Section**

Figure 1: Specimen configuration (unit: mm)

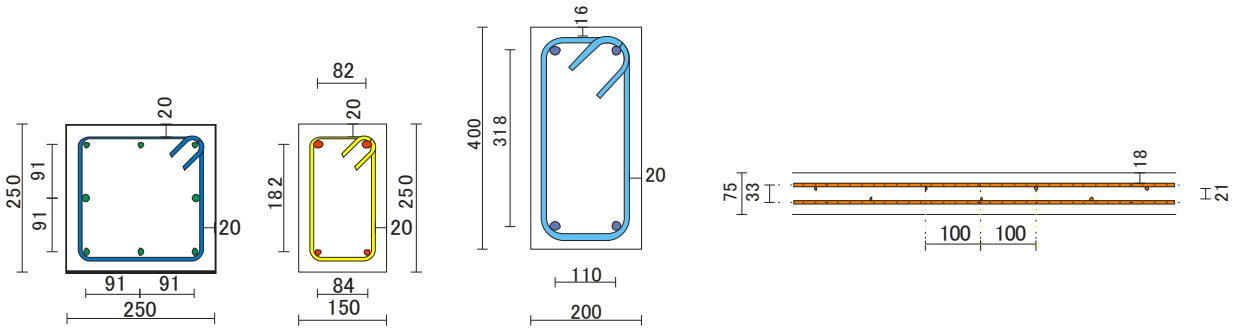

(a) column **(b) Beam** **(c) Foundation beam** **(d) Structural wall**

Figure 2: Section configurations and bar arrangement (unit: mm)

Table 1: Material properties

(a) Concrete

Compression strength (MPa)	Young's modulus (Gpa)	Tensile strength (MPa)
26.2	22.6	2.1

(b) Reinforcement

Type		Yield strength (MPa)	Young`s modulus (GPa)	Tensile strength (MPa)
D22		379	181	573
D16		345	190	502
D13		357	189	509
D10		357	188	506
D6	Vertical reinfocement of wall	382	177	531
	Other Locations	338	184	543

Table 2: Types of reinforcement

Menber	Type of bar		Steel ratio (%)
Column (250mm × 250mm)	Longitudinal	8-D10	0.913
	Transverse	2-D6@80	0.283
Boundary Column (250mm × 250mm)	Longitudinal	8-D13	1.62
	Transverse	2-D6@80	0.283
Beam (250mm × 250mm)	Upper longitudinal	2-D13	0.782
	Lower longitudinal	2-D10	0.44
	Transverse	2-D6@100	0.377
Foundation Beam (250mm × 250mm)	Upper longitudinal	2-D16	0.554
	Lower longitudinal	2-D16	0.554
	Transverse	2-D10@100	0.713
Wall (250mm × 250mm)	Vertical	D6@100	0.377
	Horizontal	D6@100	0.377

2.2. Test Setup

Figure 3 shows the loading system. Lateral load was applied statically to the mid-span of the loading beam through two horizontal 1MN hydraulic jacks. Three vertical hydraulic jacks were attached to each column top to apply the assumed gravity load. To represent dead load plus service load, 163kN (10.0%), 297kN (18.1%) and 219kN (13.3%) were applied to the east column, the central column and the west column, respectively. The values in the parentheses indicate the ratio of the axial load to $f'_c \times D^2$, where D denotes the width of the square column. Axial load on each column in Fig. 3 was kept constant during the test.

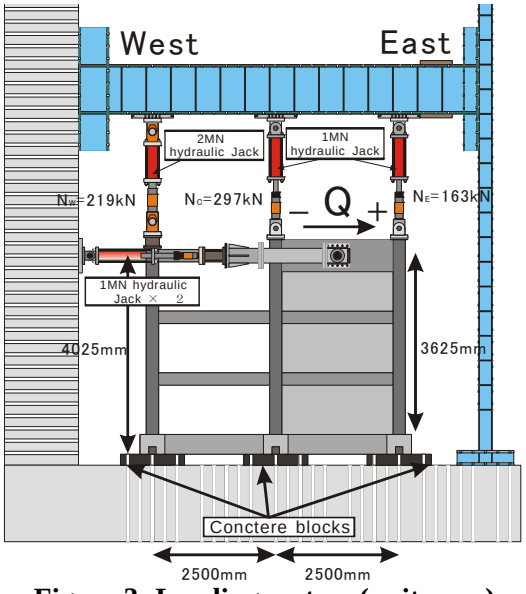

Figure 3: Loading system (unit: mm)

2.2.1 The first loading stage

The specimen was placed on concrete blocks without any anchorage to make the specimen free to be uplifted at the base. The friction at the bottom surfaces of the specimen was large enough to prevent slip from an early stage of loading. The concrete blocks were fixed to the reaction floor rigidly with prestressing bars.

In the first stage, where the specimen was not anchored to the concrete blocks, the sliding of the specimen was not observed. The coefficient of friction was estimated to be more than 0.49, judging from the ratio of the maximum horizontal load applied to the total vertical load on the concrete blocks. The specimen was loaded two cycles each at the drift angle $\gamma = \pm 0.1\%$, $\pm 0.2\%$, $\pm 0.4\%$, $\pm 0.6\%$, $\pm 0.8\%$, where the drift angle, γ, was calculated as Eq.(1). Before $\gamma = 0.8\%$, lateral loads reached the maximum values on each direction and the first loading stage was terminated.

$$\gamma = \frac{U_L}{h} \qquad (1)$$

U_L: Relative horizontal displacement between the loading beam and the foundation beam

h: Height of the loading point from the top surface of the stub (3625mm).

2.2.2 The second loading stage

After the first loading stage, the foundation stabs were fixed to the concrete blocks rigidly with prestressing bars to simulate the fixed end condition without rocking. The same displacement control procedure was used like the first loading stage. Structural wall yielded in flexure at $\gamma = +0.28\%$. After $\gamma = 1.0\%$, the specimen was loaded monotonically up to $\gamma = 2.0\%$ in positive direction to observe the shear failure.

3. TEST RESULTS

3.1. Observed Damage

Figure 4 shows the crack distributions. During the first loading stage, most of the flexural cracks were observed at the beam-ends in each story and the bottom of the external first story column of the adjacent frame, while the structural wall had few cracks. During the second loading stage, flexure-shear cracks were observed on each story of the structural wall from γ =+0.0017%. At γ =2.0% in positive direction, shear sliding failure occurred along the horizontal cracks near the compression column, which is circled by a dotted line in Figure 4 (b). It caused the reduction of the lateral load carrying capacity dramatically and the second loading stage was terminated.

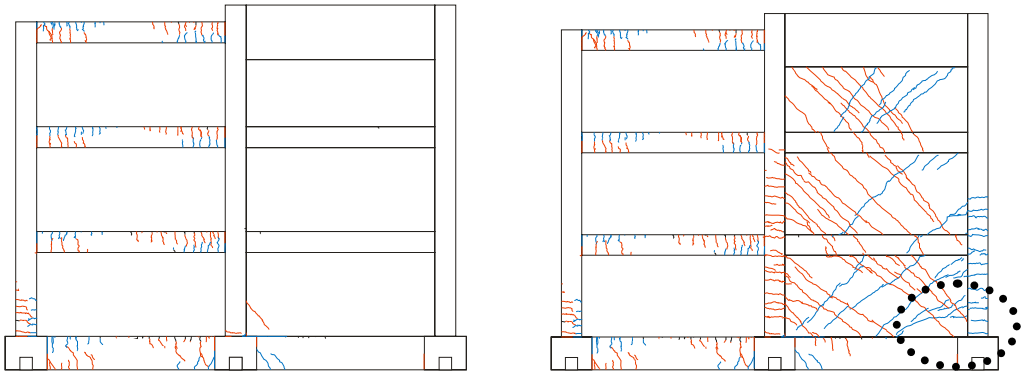

(a) The first loading stage (γ =0.8%) **(b) The second loading stage (γ =1.0%)**

Figure 4: Crack Distributions

3.2. Lateral Load-Drift Angle (γ) Relation

Figure 5 shows lateral load–drift angle (γ) relations where the drift angle, γ, is defined by Eq. 1.

The hystresis loops for the first loading stage was significantly pinched and showed a flag shape. In other words, for the loading range where no uplift was observed, the load-drift angle relation was nonlinear-elastic and the residual drift was negligible. When the lateral load were increased to reach the overturning capacity of the specimen, the most critical stub lifted up and rocking of the structural wall took place leading to a dramatic degradation of the stiffness. The structure dissipated a certain amount of energy in the loading range where the rocking motion was taking place. Thus, the resulting load-drift angle relation was a flag shape in both positive and negative direction. The enclosed area and the shape of the flag loops in positive and negative directions are different. This can be attributed to the difference of the rocking modes shown in Fig. 6. In either direction, one of the stubs under the wall was lifted up when the overturning moment reached a certain value. Then the beams of the adjacent frame are enforced to deform to follow the rocking motion of the wall. However, the enforced deformation differed depending on the loading direction as shown in Figure 7. In this figure, the drift angle at the height of loading point is shown separately for the structural wall and adjacent frame. The drift of the structural wall, γ'_{wall}, is calculated as δ'/h' ,see Fig.7. The drift of the adjacent frame, γ'_{frame}, is calculated as δ''/h' , as shown in Fig.7. Hence the drift angles of γ'_{wall} and γ'_{frame} indicate the deformation angle of the structural wall and adjacent frame respectively, which were obtained by eliminating the contribution of the rocking motion. It is clear that the structural wall is stiff and linear in either direction, hence its lateral deformation characteristics were almost independent from the loading direction. However, the drift angle of adjacent frame, γ'_{frame}, differed in positive and negative directions. The drift angle, γ'_{frame}, in positive direction is two times as large as the corresponding drift angle, γ, in Figure 5 whereas the drift angle, γ'_{frame}, in negative direction is about the same magnitude as γ. This means that the adjacent frame was enforced to deform twice as large in the positive direction as in the negative direction when the same magnitude of drift angle $|\gamma|$ was given to the structure. This explains the fact that the damage of the adjacent frame was larger in positive direction. In

addition, the energy was dissipated only at the beams and columns of the adjacent frame after the rocking motion took place and this explains the flag shape loops in Figure 5(a).

In the second loading stage, flexural cracks and flexural yielding of the structural wall caused the reduction of the stiffness of load-drift angle relation of the overall structure. Lateral load increased slowly before the shear failure of the structural wall occurred. The yield strengths of the structural wall in positive and negative directions were different. Like the first loading stage, this can be attributed to the difference of the vertical load applied at each column and the difference of the constraint of the adjacent frame.

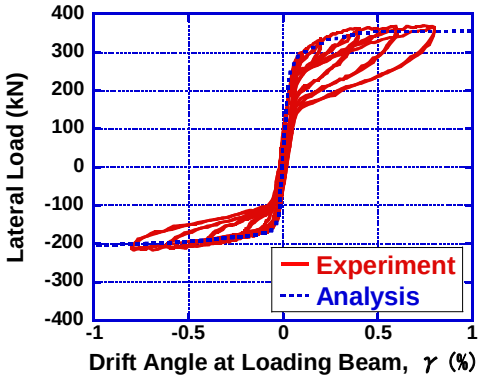

(a) The first loading stage

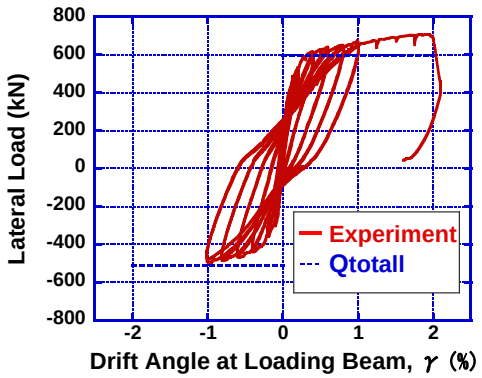

(b) The second loading stage

Figure 5: Lateral load –drift angle (γ) relation

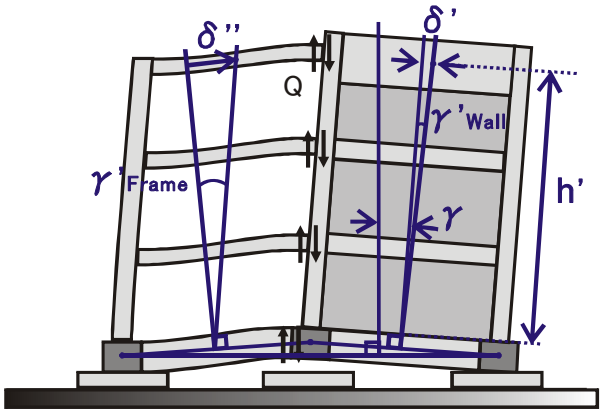

(a) Positive direction

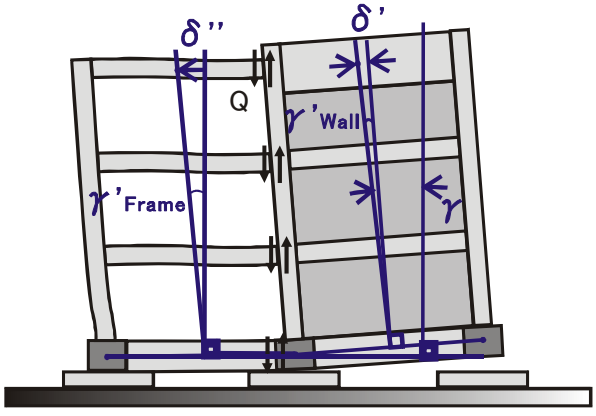

(b) Negative direction

Figure 6: Foundation uplifting mechanism

3.3. Equivalent Viscous Damping

Figure 8 shows the equivalent viscous damping in the first and the second loading stages. The equivalent viscous damping was calculated with Eq. (2) based on the second loops in each direction. The equivalent viscous damping in the first loading stage was smaller than that in the second loading stage. But as is clear from Fig. 5, residual deformation in the first loading stage was much smaller than that in the second loading stage.

$$h_{eq} = \frac{1}{4\pi}\frac{\Delta W}{W} \qquad (2)$$

ΔW : The area of steady loop

W : The area of ΔOAB in Figure 8 (c).

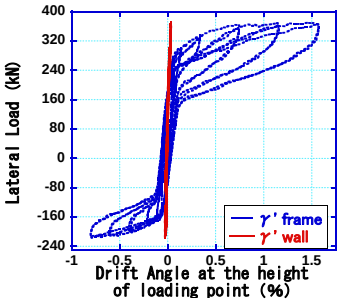

Figure 7: Lateral load-deformation angle, (γ'_{wall}, γ'_{frame}) relation

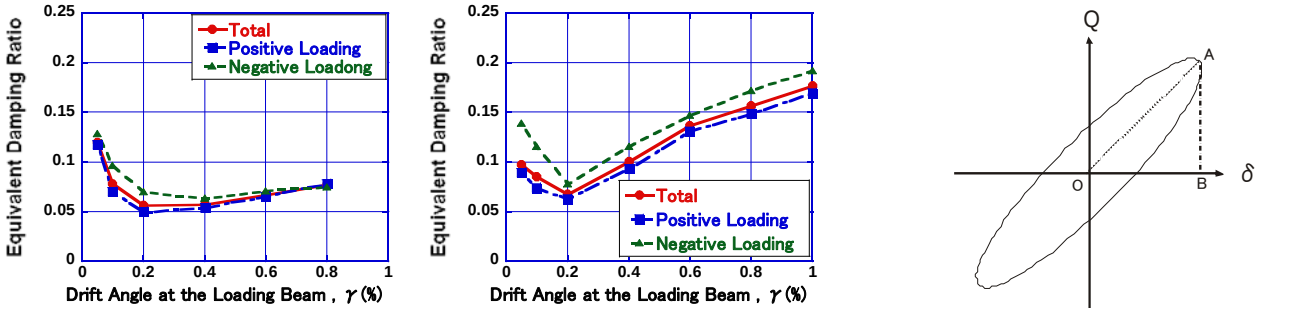

(a) The first loading **(b) The second loading** **(c) Equivalent viscous damping**

Figure 8: Equivalent viscous damping ratio

4. SIMULATION OF RESTORING FORCE CHARACTERISTICS AND DAMAGE

4.1.Analytical Model

In order to simulate the damage progress in detail, a pushover analysis was carried out using the nonlinear SAP2000 program [9], where modelling of the uplifting behavior of the specimen was also conducted.

The adjacent frame and the structural wall were modeled with beam elements. For the adjacent frame, plastic hinges were introduced at both element ends of each element.

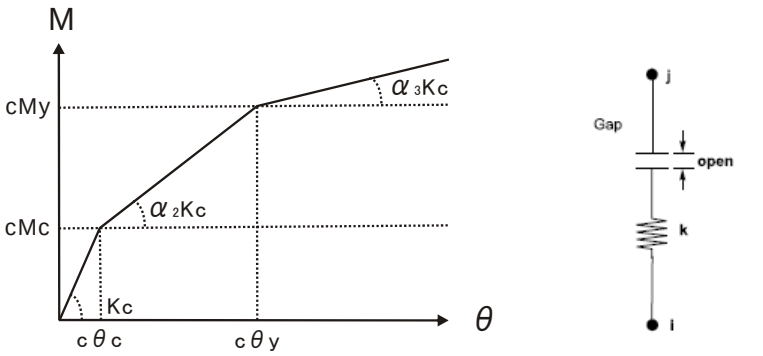

(a) Plastic hinge model for column **(b) Gap element**

Figure 9: Models for analysis

The moment-rotation characteristics of the plastic hinge were determined according to the Japanese design guidelines [3]. A schematic representation of the tri-linear plastic hinge model used for column is shown in Figure 9 (a). The column-beam joint was assumed to be perfectly rigid.

According to the Japanese design guideline [3], the structural wall was modelled with columns, braces and rigid beams. The section area of modelled columns was determined in such a way that the flexural stiffness of modelled columns was the same as that of structural wall of the specimen. Pinned supports were introduced at each column end. The section area of braces was also modelled considering the contribution of the foundation beam in such a way that the shear stiffness of this model was the same as that of structural wall. These elements were set elastic because the damage of the structural wall was negligible in this experiment.

In order to simulate foundation uplift, gap (compression-only) element was used. On condition that spring constant k is set to be infinitely large, it has the same property as a pin support under compression. But, under tension, deformation in the axis direction of the gap element is allowed and the stiffness to the axial direction is zero. This gap element was placed at the mid-span and both ends of each foundation under the structural wall as shown in Figure 10 (a).

In the second loading stage, the maximum strength, Q_{total}, was calculated as Eq. (3) in each direction. In order to calculate the maximum overall strength, the strengths of the adjacent frame and the structural wall were calculated separately. The adjacent frame was calculated with the moment-distribution method. The plastic hinges were introduced as in the first loading stage. The strength of the structural wall was calculated by Eq. (4) considering of the vertical load applied at each column and shear force from the 2F, 3F and 4F beams acting on

the structural wall as axial force. Since the value of axial load, N, depends on direction, the maximum strength, Q_{total}, in positive direction was different from that in negative direction.

$$Q_{total} = \begin{Bmatrix} Q^{+}{}_{column} + Q^{+}{}_{wall} \\ Q^{-}{}_{column} + Q^{-}{}_{wall} \end{Bmatrix} \quad (3)$$

$${}_{w}M_{y} = a_t \sigma_y l_w + 0.5 \sum \left(a_w \sigma_{wy} \right) l_w + 0.5 N l_w \quad (4)$$

4.2. Comparison between Computed and Experimental Results

Table 3 shows the comparison between the computed and experimental results in the first loading stage. Cracking load points in the first loading stage could not be predicted well. Cracks were formed earlier in experiment than in analysis. This caused the overestimate of the stiffness for the stage before foundation uplifting in the analysis. As to the load when foundation uplifting occurred, analytical result agreed well with the experimental result. After foundation uplift, the shape of the envelope curves was accurately simulated.
The straight lines in Figure 5(b) showed the calculated maximum strength of the specimen in second loading stage. In positive direction, the analysis underestimated the maximum strength in experiment. In negative direction, the maximum strength in experiment agreed with the calculated one.

Table 3. Characteristic points in the first loading stage

(a)Experiment

	Load (kN)		Drift Angle (%)	
	Positive	Negative	Positive	Negative
Crack	50	50	0.0017	0.0052
Uplift	273	148	0.0610	0.0519
Maximum	369	216	0.613	0.770

(b) Analysis

	Load (kN)		Drift Angle (%)	
	Positive	Negative	Positive	Negative
Crack	250	159	0.0363	0.0541
Uplift	241	140	0.0316	0.0300
Maximum	354	201	0.803	0.803

Analytical maximum values of the first loading were calculated on condition that γ was 0.8%.

4. CONCLUSIONS

One 40% scaled specimen consisting of a multi-story structural wall and an adjacent frame was tested. In the first loading stage, the foundation was not fixed and foundation uplift was permitted. In the second loading stage, the foundation was rigidly fixed to the testing reaction floor. This study aims to clarify the effects of the uplift of wall base foundation on the restoring force characteristics, energy dissipation capacity, etc, focusing on such dual structural system. Also investigated was whether existing damage evaluation procedures were applicable to the experimental results or not. The main conclusions are summarized as follows.

- In the first loading stage, foundation uplift was observed. Damage of the specimen concentrated on the adjacent frame. There were few cracks on the structural wall. In the second loading stage, the foundation was fixed rigidly to the testing reaction floor. The structural wall failed in shear after flexural yielding of the structural wall.
- Comparing the first loading stage and the second loading stage, lateral strength in the first loading stage was almost 50% of that in the second loading stage in both loading directions. Equivalent viscous damping in the first loading stage was almost 50% of that in the second loading stage at γ =0.8%. But residual displacement in the first loading stage was much smaller than that in the second loading stage.
- Restoring force characteristic in the first loading stage was simulated well with the nonlinear SAP2000 program. In the analysis, plastic hinge models according to the Japanese guideline and gap elements for simulating foundation uplift were used.
- Maximum load stage was calculated with moment-distribution method for the second loading stage. In positive direction, the calculated value underestimated the measured maximum strength, but in negative direction the calculated strength agreed well with the observed maximum strength in experiment.

5. ACKNOWLEDGEMENT

A part of this research was financially supported by the Special Project for Earthquake Disaster Mitigation in Urban Areas, Ministry of Education, Culture, Sports, Science and Technology (PI: H. Tanaka)

REFERENCES

[1] Chad Harden, Tara Hutchinson and Mark Moore (2006). Investigation into the effects of foundation uplift on simplified seismic design procedures. Earthquake Spectra Volume 22 No.3: 663-692.
[2] American Society of Civil Engineers (ASCE), 2000. Prestandard and Commentary for the Seismic Rehabilitation of buildings, prepared for the Federal Emergency Management Agency, FEMA-356, Washington , D.C)
[3] Architecture Institute of Japan (2001). Design Guidelines for Earthquake Resistant Reinforced Concrete Buildings Based on Inelastic Displacement Concept (In Japanese)
[4] Hayashi, Y., (1996). Damage reduction effect due to basemat uplift of buildings. Journal of Structural and Construction Engineering AIJ No.485: 53-62 (in Japanese)
[5] Katsumata, H., Kato, D., Aoyama, H., Otani, S., (1981). A study on frames with a uplifting shear wall (Part1, Part2). Summaries of technical papers of annual meeting, AIJ: 1671-1674 (in Japanese)
[6] Saito, T., Teshigawara, M., Fukuyama, H.,Kato, H., Kusunoki, K., Mukai, T. and and Kabeyasawa, T. (2004). Simulation of nonlinear behavior of reinforced concrete wall-frame structures under earthquake loads. 13th World Conference on Earthquake Engineering. Vancouver. Canada. pdf.No.1561
[7] Kato, A., Kabeyasawa, T., Kajiwara, K.,Matsumori, T. and Kuramoto, H. (2004). Earthquake simulation test of reinforced concrete wall frame structure with rocking or uplifting foundation. Journal of Structural Engineering AIJ Vol.50B: 119-125 (in Japanese)
[8] The Building Center of Japan (1999). Design and Construction Guidelines for Multiple Story Frame Structures with Shear Wall (In Japanese)
[9] Computers and Structures (2002). SAP 2000 Integrated Software for Structural Analysis and Design ANALYSIS REFERENCE MANUAL: 209-210
[10] Architecture Institute of Japan (2004). Guidelines for Performance Evaluation of Earthquake Resistant Reinforced Concrete Buildings (Draft) (In Japanese)